

CINO₂ Production from N₂O₅ Uptake on Saline Playa Dusts: New Insights into Potential Inland Sources of CINO₂

Dhruv Mitroo,[†] Thomas E. Gill,[‡] Savannah Haas,[§] Kerri A. Pratt,[§] and Cassandra J. Gaston^{*,†}

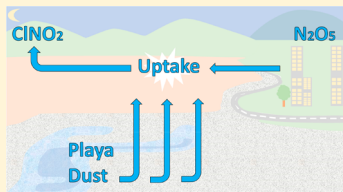
[†]Department of Atmospheric Sciences, Rosenstiel School of Marine & Atmospheric Sciences, University of Miami, Miami, Florida 33149, United States

[‡]Department of Geological Sciences, and Environmental Science and Engineering Program, University of Texas at El Paso, El Paso, Texas 79968, United States

[§]Department of Chemistry, University of Michigan, Ann Arbor, Michigan 48109, United States

Supporting Information

ABSTRACT: Nitryl chloride (ClNO₂), formed when dinitrogen pentoxide (N₂O₅) reacts with chloride-containing aerosol, photolyses to produce chlorine radicals that facilitate the formation of tropospheric ozone. CINO₂ has been measured in continental areas; however, the sources of particulate chloride required to form ClNO₂ in inland regions remain unclear. Dust emitted from saline playas (e.g., dried lakebeds) contains salts that can potentially form ClNO₂ in inland regions. Here, we present the first laboratory measurements demonstrating the production of ClNO₂ from playa dusts. N₂O₅ reactive uptake coefficients (γ_{N2O5}) ranged from $\sim 10^{-3}$ to 10^{-1} and CINO₂ yields (φ_{CINO2}) were $> 50\%$ for all playas tested except one. In general, as the soluble ion fraction of playa dusts increases, γ_{N2O5} decreases and φ_{CINO2} increases. We attribute this finding to a transition from aerosol surfaces dominated by silicates that react efficiently with N₂O₅ and produce little ClNO₂ to aerosols that behave like deliquesced chloride-containing salts that generate high yields of ClNO₂. Molecular bromine (Br₂) and nitryl bromide (BrNO₂) were also detected, highlighting that playas facilitate the heterogeneous production of brominated compounds. Our results suggest that parameterizations and models should be updated to include playas as an inland source of aerosol chloride capable of efficiently generating ClNO₂.



1. INTRODUCTION

Reactive halogens are potent oxidizers that influence the earth's climate and air quality by reducing the lifetime of methane (CH₄) and affecting budgets of tropospheric ozone (O₃), a greenhouse gas and criteria air pollutant.^{1,2} The chlorine radical (Cl[·]) is a reactive halogen that is efficient at oxidizing volatile organic compounds (VOCs), augmenting tropospheric O₃ production,^{3–9} and facilitating the formation of secondary organic aerosol (SOA).¹⁰ In urban environments, the most common precursor to Cl[·] is nitryl chloride (CINO₂).^{11–13}

CINO₂ is produced following the heterogeneous reaction of dinitrogen pentoxide (N₂O₅), a nighttime reservoir for nitrogen oxides (NO_x) in polluted environments, on chloride-containing aerosols.¹¹ N₂O₅ is taken up onto aerosols with an efficiency referred to by the reactive uptake coefficient (e.g., γ_{N2O5}), which is the probability that colliding N₂O₅ molecules undergo irreversible reaction on or in a particle. N₂O₅ has been shown to react with deliquesced inorganic salts with values of γ_{N2O5} ranging from 0.015 to 0.2 from laboratory studies^{14–23} as well as field work (e.g., McDuffie et al. 2018a and references therein).^{13,24–32} Upon solvation, N₂O₅ is proposed to form a nitrate ion (NO₃[−]) and a hydrated intermediate (H₂ONO_{2(aq)}⁺), which can further react with water to form nitric acid (HNO₃).³³ However, in the presence of aqueous chloride (Cl^{−(aq)}), the H₂ONO_{2(aq)}⁺ intermediate can react to produce CINO_{2(aq)}.^{11,13,14,34} The rate constant for

the reaction of the N₂O₅ intermediate with Cl^{−(aq)} has been estimated to be a factor of 500–800 larger than the reaction with H₂O, causing even small concentrations of Cl^{−(aq)} in aerosols to influence the product yield.^{14,22,34} CINO_{2(aq)} volatilizes and photolyses to produce atomic chlorine (Cl[·]) while recycling a nitrogen dioxide (NO₂) molecule.³⁵ The photolysis of CINO₂ is estimated to contribute significantly to the total tropospheric Cl[·] budget, and therefore it is critical to constrain sources of aerosol chloride.^{2,36}

CINO₂ production in coastal regions has been widely reported both from field observations^{2,12,32,36–42} and laboratory measurements using salt solution mimics.^{14,22,23,42,43} This process has now been accepted as a major pathway for the production of CINO₂,^{2,44} however, recent field measurements show elevated CINO₂ mixing ratios in continental regions,^{13,25–27,29–31} suggesting that sources of chloride-containing aerosol other than sea spray aerosol can also produce CINO₂. Potential sources of particulate chloride that can facilitate the inland production of CINO₂ include biomass burning aerosol,⁴⁵ road salts,⁴⁶ and industrial emissions from coal-fired power plants.^{27,31,47} However, other under-explored yet potentially important sources of particulate chloride found

Received: February 21, 2019

Revised: May 17, 2019

Accepted: May 22, 2019

Published: May 22, 2019

inland are drying saline lake beds (playas). Evaporite minerals (e.g., salts) associated with playas, including halite (NaCl), are derived from saline groundwater or dissolved minerals in surface waters that evaporate, leaving behind a salt-rich, erodible crust that can be mobilized as dust by aeolian processes and may be a significant source of chloride-containing aerosol.^{48–56} Playas, in North America and globally, are disproportionately potent emitters of dust aerosols.^{57,58} Gaseous halogen oxides (e.g., ClO and BrO) have been observed over playas including the Great Salt Lake,⁵⁹ Salar de Uyuni,⁶⁰ and the Dead Sea;⁶¹ suggesting that playa surfaces can participate in halogen chemistry. Additionally, crustal aerosol originating from playas in the southwestern United States was suggested to indirectly contribute to the formation of ClNO_2 during the Nitrogen, Aerosol Composition, and Halogens on a Tall Tower (NACHTT) campaign through the acid displacement of supermicron particulate chloride leading to the formation of hydrochloric acid (HCl) that partitions to submicron particles and facilitates the production of ClNO_2 .^{62–64} However, the direct production of ClNO_2 from saline playas has never been measured.

Here, we present the first laboratory measurements of the reactive uptake of N_2O_5 and yield of ClNO_2 at different relative humidities (RHs) from saline playa dusts collected from southwestern North America. We show that all playa dusts tested, except one, generated ClNO_2 at significant yields and that some generated brominated products. We end with a discussion of the implications of our work for updating current parameterizations of the formation of ClNO_2 in inland regions.

2. MATERIALS AND METHODS

2.1. Generation of Playa Dust Particles. Surface samples were obtained from seven saline playas in southwestern North America that are known dust emitters: Black Rock Desert (Nevada),^{65–68} Great Salt Lake (Utah),⁶⁹ Lordsburg Playa (New Mexico),^{70,71} Owens (dry) Lake (California),^{72–74} Salt Flat Basin (Texas),⁷⁵ Salton Sea (California),⁷⁶ and Sulphur Springs Draw (Texas).^{77,78} Two samples from Owens Lake collected on the same day were used in this study: the first sample was a white, hard salt “crust”,⁴⁸ and the second sample was a soft, sand-silt-clay “sediment”.⁴⁸ Photos of these two samples are available in Figure S1 of the Supporting Information (SI). Coordinates for all samples and additional information on the playas and their characteristics are available in Figure S2 and Table S1. All of the playa sediment samples were used “as is” except for the sample obtained from the Great Salt Lake, which was dried at 45 °C for 48 h.

Our custom dry aerosol generation set up, described in the SI, includes a mechanical agitation method using a wrist action shaker similar to other dry aerosol generation systems.⁷⁹ The output was conditioned in a ~19 L dilution drum,⁸⁰ and supermicron particles were removed using a cyclone (Mesalabs) with a PM_1 (particles with aerodynamic diameter $>1 \mu\text{m}$) cutoff. We chose to restrict our study to submicron aerosols that are most susceptible to long-range transport⁸¹ and would have a larger spatial impact on halogen activation. Following the cyclone, excess charge was eliminated using a ^{210}Po neutralizer.⁸² A humidified dilution flow of ultrahigh purity N_2 (~5 L min⁻¹) was introduced to condition the RH of the dust-laden flow, which was measured using a humidity probe (model HMP60; Vaisala) just prior to the entrance of the aerosol flow tube (AFT) to ensure that the aerosol was fully conditioned to the expected RH. The humidity in the

AFT for our experiments ranged from 10–60% RH. The aerosol concentration was stable for up to ~15 min using this set up, longer than a typical uptake duration of ~10 min.

2.2. Aerosol Kinetics Flow Tube Set Up. Our experimental setup is depicted in Figure S3. Generated aerosols orthogonally entered a 90 cm long, 6 cm inner diameter Pyrex AFT coated with halocarbon wax (Halocarbon Corp.) to minimize wall losses. N_2O_5 was generated continuously in a Teflon vessel by first forming NO_3 by reaction of NO_2 (10 ppm standard; Airgas) and O_3 generated with a UV-pen lamp (Jelight Model 610). NO_3 was then allowed to react further with excess NO_2 to produce N_2O_5 in equilibrium with NO_2 and NO_3 at room temperature.^{15,22,42,83,84} The final flow was ~0.1 L min⁻¹, which was introduced via a Teflon lined stainless steel movable injector along the centerline of the AFT. We utilized the central 50 cm as the reaction zone to ensure fully developed laminar flow. N_2O_5 , ClNO_2 , Br_2 , BrNO_2 , and other halogenated species were detected using an iodide-adduct chemical ionization mass spectrometer (CIMS) as $[\text{I} \cdot (\text{N}_2\text{O}_5)]^-$ (234.9 amu), $[\text{I} \cdot (\text{ClNO}_2)]^-$ (207.9 and 209.9 amu), $[\text{I} \cdot (\text{Br}_2)]^-$ (284.9, 286.9, and 288.9 amu), and $[\text{I} \cdot \text{BrNO}_2]^-$ (251.9 and 253.9 amu) with isotope ratios confirming assignment of our ion peaks.^{42,85} Additional details of this instrument are available in the SI. The humidified total particle surface area was measured at the exit of the AFT after the aerosol had been humidified using a scanning mobility particle sizer (SMPS; model 3082, TSI, Inc.) and an aerosol particle sizer (APS; model 3321, TSI, Inc.). To ensure that the measured particle surface area was representative of humidified conditions during experiments in the AFT, both instruments sampled humidified flow for ~1 h prior to the start of the experiment in order to equilibrate the RH of the DMA sheath flow. To preserve the laminar regime in the AFT, the APS sample flow was diluted by a factor of ~10. Figure S4 shows a typical size distribution observed during our work.

2.3. Determination of $\gamma_{\text{N}_2\text{O}_5}$ and Yields of ClNO_2 . We determined the reaction probability of N_2O_5 , $\gamma_{\text{N}_2\text{O}_5}$, via particle modulation.⁸³ At a fixed injector position, we modulated the dust output through the AFT in ~15 min intervals; this allowed ~5 min for steady-state conditions to develop in the reaction zone where aerosols and N_2O_5 interacted followed by ~10 min of averaging signal. The N_2O_5 signal was determined in the presence of both reactor walls and aerosols and then reactor walls alone; thus the pseudo-first-order rate constant for N_2O_5 loss, k_{het} , was calculated using eq 1⁸³

$$k_{\text{het}} = -\frac{1}{\Delta t} \ln \frac{[\text{N}_2\text{O}_5]_{w/\text{aerosol}}}{[\text{N}_2\text{O}_5]_{w/o \text{ aerosol}}} \quad (1)$$

where Δt is the reaction time, $[\text{N}_2\text{O}_5]_{w/\text{aerosol}}$ is the N_2O_5 signal in the presence of aerosol, and $[\text{N}_2\text{O}_5]_{w/o \text{ aerosol}}$ is the N_2O_5 signal in the absence of aerosol. The reactive uptake coefficient, $\gamma_{\text{N}_2\text{O}_5}$, was then calculated using eq 2

$$\gamma = \frac{4k_{\text{het}}}{\omega S} \quad (2)$$

where ω is the mean molecular speed of N_2O_5 and S is the aerosol total surface area concentration. For each experiment, we repeated this procedure five times at every humidity using different particle surface areas, which produced linear correlations (<10% error by weighted least-squared fits) between k_{het} and S (see Figure S5). Values of $\gamma_{\text{N}_2\text{O}_5}$ were

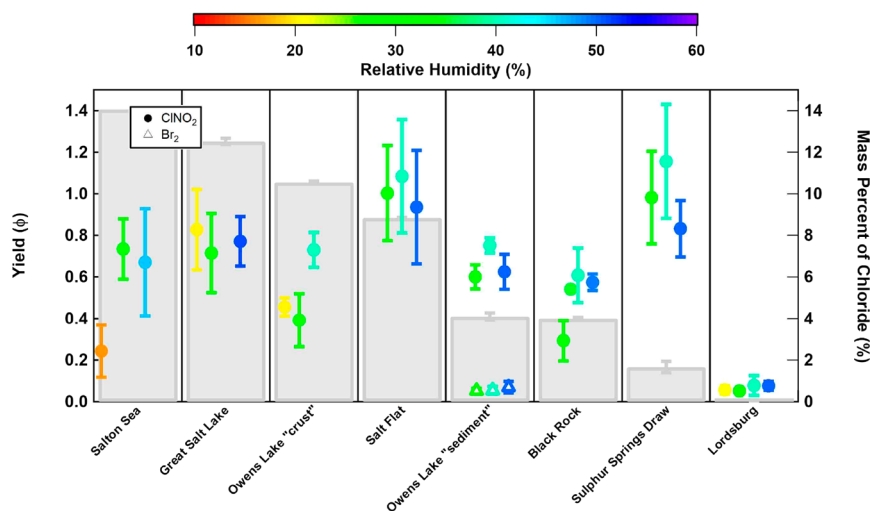


Figure 1. Yields of ClNO_2 and Br_2 for playa samples determined at different humidities (left axis) displayed in order from highest chloride content (left) to lowest chloride content (right). Error bars represent one standard deviation between repetitions. Markers are colored based on the RH for which the yield values were determined. Gray bars (right axis) correspond to the sample chloride content, measured via IC.

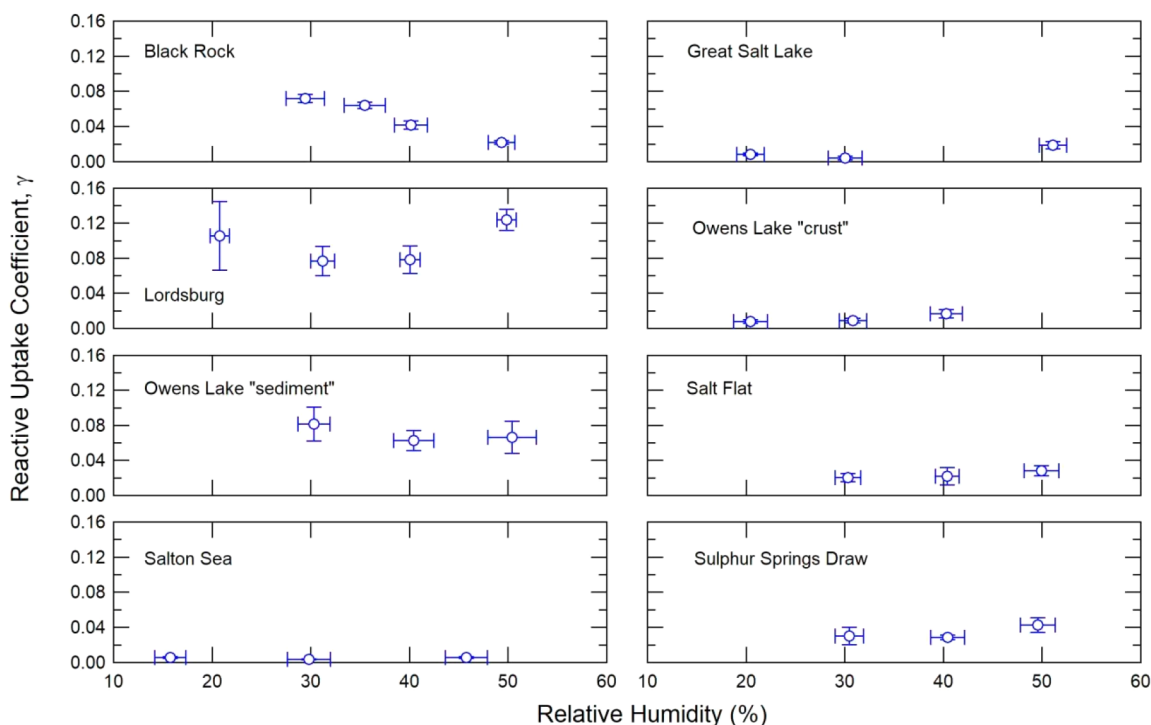


Figure 2. Reactive uptake coefficients, γ , of N_2O_5 on different playa samples are shown as a function of RH. Vertical error bars represent $\pm 1\sigma$ of 5 repetitions at each RH.

then corrected for gas-phase diffusion limitations⁸⁶ (<5% error) and non plug flow conditions⁸⁷ using a wall loss measurement that was made at the end of each run (~10% error).

The largest correction to our measurements was the determination of S . Corrections based on aerosol density and shape were applied,⁸⁸ details for which can be found in the SI. The playa samples used in our experiments are not composed solely of silicate minerals typical of most mineral dust; rather, they are a combination of silicate minerals and significant amounts of evaporites. To account for the density contributions of silicate minerals and evaporite salts, we measured the soluble ion content of the playa samples using ion

chromatography (IC) (see Table S2 and information in the SI). We attribute the soluble ions to evaporite mass (density $\sim 1.3 \text{ g cm}^{-3}$)⁸⁹ and the remainder of our sample mass to silicates (density $\sim 2.7 \text{ g cm}^{-3}$),⁹⁰ an assumption based on previous dust measurements.⁵⁵ Taking these corrections into account, we estimate that the APS overpredicts S by $\sim 20\text{--}40\%$ on average (see Table S2). Uncorrected values of $\gamma_{\text{N}_2\text{O}_5}$ and corrected values of $\gamma_{\text{N}_2\text{O}_5}$, referred to as γ_{true} , are shown in Table S3.

The yield of ClNO_2 (φ_{ClNO_2}) is defined as the amount of ClNO_2 produced per amount of N_2O_5 reacted. Yields of ClNO_2 were determined by performing routine calibrations for the sensitivity of ClNO_2 relative to N_2O_5 by flowing N_2O_5 over

a wetted NaCl slurry, which theoretically produces ClNO₂ with a yield of unity for fully deliquesced aerosol.^{11,36,42} The generated ClNO₂ is then introduced to a stream of humidified air to calibrate the response of the CIMS to N₂O₅ and ClNO₂ at different RHs. We also calibrated the CIMS to Cl₂ and Br₂ using permeation tubes with known emissions rates (74 and 65 ng min⁻¹ certified emission rate at 40 °C by KIN-TEK, respectively) and varied the flow rate into the carrier gas stream to test the instrument response to different additions of Cl₂ and Br₂. To report yields of Br₂ observed in this work, we estimated that ~1.8 ppb N₂O₅ was introduced to the AFT during our experiments using a collision limit calculation.⁹¹ This gave us an upper limit for the instrument sensitivity to N₂O₅ (~18 Hz ppt⁻¹ for every MHz of total reagent ion signal) and thus a lower limit for the mixing ratio of N₂O₅. As a result, φ_{Br_2} values reported in this work are upper limits.

2.4. Estimating the Salt and Liquid Content of Playa Dusts. To compare the observed yields of ClNO₂ from our samples to those predicted with the current laboratory-based parameterizations, we used IC data and experiment RH conditions as inputs into ISORROPIA-II⁹² to predict the liquid water and aqueous chloride content of the aerosols as a function of RH. We chose ISORROPIA-II for its ability to handle complex mixtures, including K⁺, Mg²⁺, and Ca²⁺, which are present in non-negligible concentrations in our samples and impact the aerosol liquid water content and amount of aqueous chloride due to their highly hygroscopic nature.⁹³ Table S4 in the SI contains a complete list of measured cations and anions for each playa sample. We then used the model output to predict theoretical values for φ_{ClNO_2} using eq 3²²

$$\varphi_{\text{ClNO}_2} = \left(1 + \frac{k_{\text{H}_2\text{O}}[\text{H}_2\text{O}_{(l)}]}{k_{\text{Cl}^-}[\text{Cl}^-_{(aq)}]} \right)^{-1} \quad (3)$$

where we use a value of $k_{\text{H}_2\text{O}}/k_{\text{Cl}^-}$ of 1/483,²² but note that there is spread in this value.^{14,34}

3. RESULTS AND DISCUSSION

3.1. ClNO₂ Yields and N₂O₅ Reactive Uptake Coefficients from Saline Playa Dusts. As shown in Figure 1 and Table S3, all of the playa dust samples used in this study produced ClNO₂, with several playa dusts generating ClNO₂ at high yields ($\varphi_{\text{ClNO}_2} > 0.5$). Figure 1 is organized by decreasing chloride mass fraction, and the playas with chloride mass concentrations above 1% generate appreciable ClNO₂. Aerosols generated from each playa sample showed differing trends between RH and $\gamma_{\text{N}_2\text{O}_5}$ (Figure 2), which is consistent with previous laboratory studies that also showed that an increase in RH can increase, decrease, or have no effect on $\gamma_{\text{N}_2\text{O}_5}$ depending on the mineralogy of the aerosol.^{90,94–96} Similar values of φ_{ClNO_2} and $\gamma_{\text{N}_2\text{O}_5}$ were observed for the Sulphur Springs Draw and Salt Flat playa samples with $\varphi_{\text{ClNO}_2} \sim 1$ and $\gamma_{\text{N}_2\text{O}_5}$ ranging from 0.020 to 0.043 (Figure 2). These values are consistent with deliquesced chloride salts and match our results for a NaCl standard used as a check on our results (Table S3). Dust generated from the Great Salt Lake also produced ClNO₂ in high yields ($\varphi_{\text{ClNO}_2} \sim 0.7–0.8$); however, $\gamma_{\text{N}_2\text{O}_5}$ values were lower, in the range of 0.004–0.019, and increased with RH (Figure 2). Little variation in the values of both φ_{ClNO_2} and $\gamma_{\text{N}_2\text{O}_5}$ were observed for dust generated from the Sulphur Springs Draw, Salt Flat, and Great Salt Lake at the three RHs tested, which is surprising given that we performed

dry generation on our samples and were well below the deliquescence RH of pure NaCl (~75%).^{89,97} One possible explanation for reactive uptake below the NaCl deliquescence RH is the presence of chloride-containing evaporites other than halite (NaCl) such as magnesium chloride and/or calcium chloride that are more hygroscopic than NaCl.^{93,98} Another possible explanation for our results is the presence of hydrated salts in our samples, which are typically observed in playa and salt crust evaporites^{74,99,100} and were previously suggested to explain the observed water uptake properties for dusts generated from the Great Salt Lake and Salt Flat.⁵⁵ These hydrates and other hygroscopic minerals are the best candidates for providing aqueous chloride needed to facilitate the production of ClNO₂ at low RH from these samples.

The Owens Lake “crust” and Salton Sea samples showed increasing values of both φ_{ClNO_2} and $\gamma_{\text{N}_2\text{O}_5}$ with increasing RH. The yield of ClNO₂ increased from 0.39 to 0.73 for the Owens Lake “crust” and from 0.24 to 0.74 for the Salton Sea; $\gamma_{\text{N}_2\text{O}_5}$ increased from 0.008 to 0.017 for the Owens Lake “crust” and from 0.004 to 0.006 for the Salton Sea. The best explanation for our observations is the presence of crystalline salts at low RH that become increasingly deliquesced with increasing RH and provide aqueous chloride that is available to react with N₂O₅. Previous laboratory studies have demonstrated that $\gamma_{\text{N}_2\text{O}_5}$ and φ_{ClNO_2} are strongly dependent on particle phase,^{101–103} supporting this explanation. The Owens Lake “sediment” sample, however, was highly reactive with N₂O₅ ($\gamma_{\text{N}_2\text{O}_5} \sim 0.063$ to 0.081) and generated ClNO₂ in appreciable yields ($\varphi_{\text{ClNO}_2} \sim 0.6$ to 0.75) at all RHs tested. The different $\gamma_{\text{N}_2\text{O}_5}$ and φ_{ClNO_2} for the Owens Lake “crust” and the “sediment” reflects the different types of material that were collected and analyzed. The “sediment” sample represents a mixture of materials derived from both the evaporite surface and the salt-silt-clay crust directly underneath, including highly hygroscopic sodium carbonates and sodium sulfates⁵⁵ that best explain our high values of $\gamma_{\text{N}_2\text{O}_5}$ and φ_{ClNO_2} . In contrast, the “crust” sample was a hard, white material composed of pure salts that do not fully deliquesce at the humidities used in this work.^{50–52,74,104,105} These results underscore the heterogeneity of mineral content not only across playas but also within the same playa.¹⁰⁶

In contrast to the Salton Sea and the Owens Lake “crust” samples that show increasing values of both $\gamma_{\text{N}_2\text{O}_5}$ and φ_{ClNO_2} with RH, dust generated from the Black Rock Desert showed increasing yields of ClNO₂ (0.3–0.6) but a decrease in N₂O₅ reactivity (0.07–0.02) with increasing RH. Our values of $\gamma_{\text{N}_2\text{O}_5}$ for this sample are strikingly similar to previous work that probed the reactive uptake of N₂O₅ on illite.⁹⁵ The reaction between N₂O₅ and the hydroxyl groups (–OH) on the surface of silicates, such as illite, is thought to be more efficient than the hydrolysis mechanism resulting in high values of $\gamma_{\text{N}_2\text{O}_5}$.^{107,108} Our results for the Black Rock Desert playa are best explained by a blend of reactive aluminosilicates and evaporites where the silicates are highly reactive with N₂O₅ at low RH. As the RH increases, the evaporites provide an increasing amount of deliquesced chloride, which reduces $\gamma_{\text{N}_2\text{O}_5}$ and increases φ_{ClNO_2} with RH. High values of $\gamma_{\text{N}_2\text{O}_5}$ (~0.08 to 0.12) were also observed for the Lordsburg playa, which has been shown to contain a dominant fraction of silicates and low concentrations of hygroscopic evaporite minerals.^{55,109} In contrast to all of the other samples, the Lordsburg playa dust generated little ClNO₂ ($\varphi_{\text{ClNO}_2} \sim 0.05$ to 0.08) likely due to the lack of Cl[–] in the sample (0.06 ± 0.02

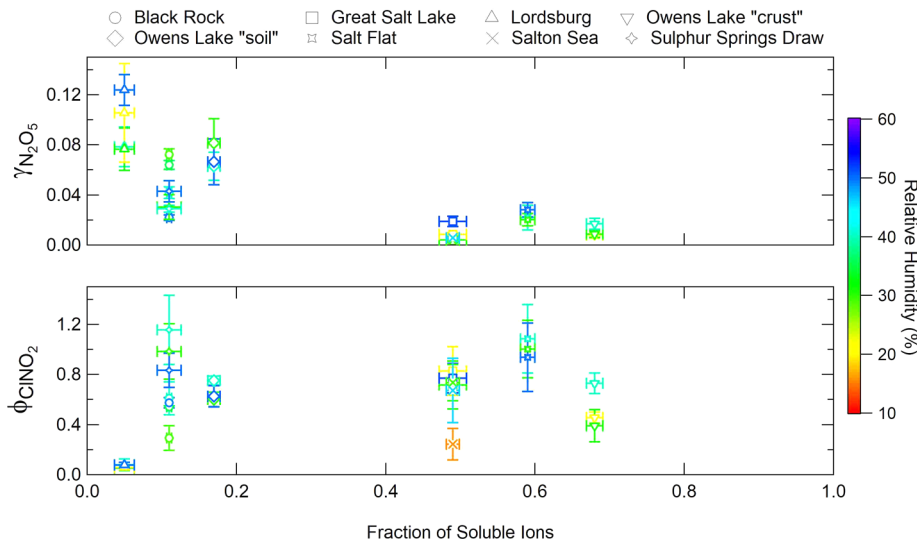


Figure 3. $\gamma_{\text{N}_2\text{O}_5}$ and ϕ_{CINO_2} are shown as a function of the soluble ion content measured by IC. Values are colored by RH. Vertical error bars represent $\pm 1\sigma$ of 5 repetitions at each RH.

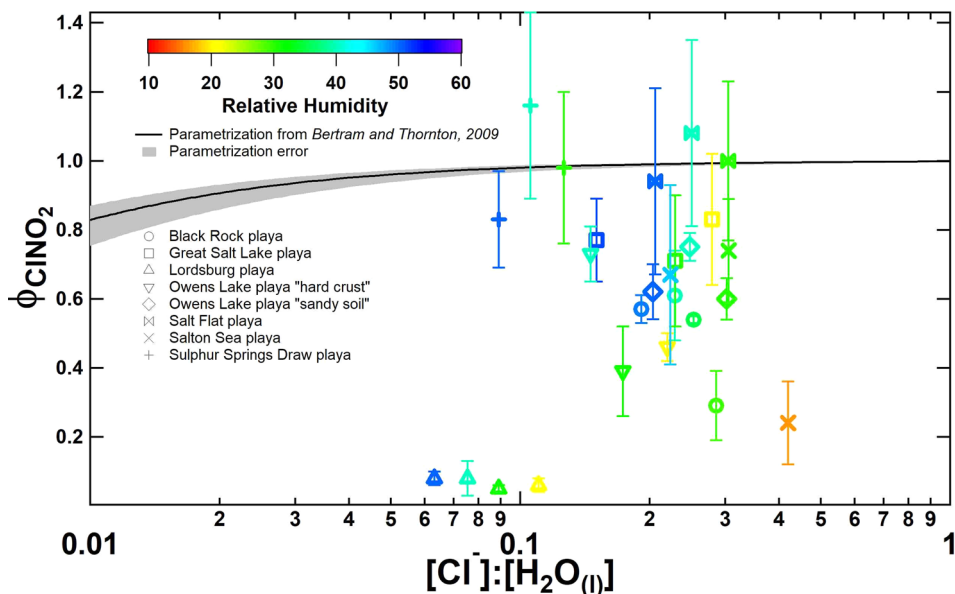


Figure 4. Measured values of ϕ_{CINO_2} plotted against the aerosol chloride-to-water ratio derived from the aqueous-phase chloride content and predicted liquid water content obtained from ISORROPIA-II, which was run in two modes: (i) solid precipitates are allowed to form (not shown) and (ii) only metastable liquid solutions are allowed to form (filled markers). Values are colored by RH. Solid line represents the parameterization by Bertram and Thornton, (2009)²² for yields of CINO_2 as a function of the aerosol chloride-to-water ratio, with shading representing the associated error.

wt %; see Figure 1 and Table S4). Altogether, these results highlight the impact of the mixed mineralogy of playas on their reactivity toward N_2O_5 and the production of CINO_2 .

3.2. Evaporite Content and Predicted Yields of CINO_2 .

In order to probe the relationship between playa dust composition, ϕ_{CINO_2} , and $\gamma_{\text{N}_2\text{O}_5}$, the measured soluble inorganic ion content (Table S4) was used to estimate the amount of evaporites associated with each playa sample. In general, playa dusts with lower mass fractions of soluble ions (e.g., evaporites) have high values of $\gamma_{\text{N}_2\text{O}_5}$, and as the soluble ion content increases, values of $\gamma_{\text{N}_2\text{O}_5}$ converge to ~ 0.02 – 0.03 , consistent with N_2O_5 uptake on deliquesced inorganic salts observed in laboratory studies (see Figure 3).^{14,15,21–23,42,110,111} Conversely, ϕ_{CINO_2} generally increased with increasing fractions of soluble ions until plateauing at

$\sim 50\%$ soluble fraction (corresponding to approximately $>5\%$ chloride by mass in Figure 1).

The decreasing trend in $\gamma_{\text{N}_2\text{O}_5}$ and increasing trend in ϕ_{CINO_2} with increasing evaporite content, shown in Figure 3, reflects the competition between silicates and evaporites for N_2O_5 and the impact of this competition on the reaction products formed. Samples with low evaporite content (<20%) have a large mass fraction of silicates that react efficiently with N_2O_5 resulting in high values of $\gamma_{\text{N}_2\text{O}_5}$.^{95,107,108} For these samples, the scarcity of soluble ions, including chloride (Figure 1), coupled with previous observations of the formation of absorbed nitrates when N_2O_5 reacts with silicates¹⁰⁸ best explain the low yields of CINO_2 from samples with very low soluble ion (evaporite) content. Conversely, samples with high evaporite content ($\geq 50\%$) behave similarly to deliquesced, chloride-

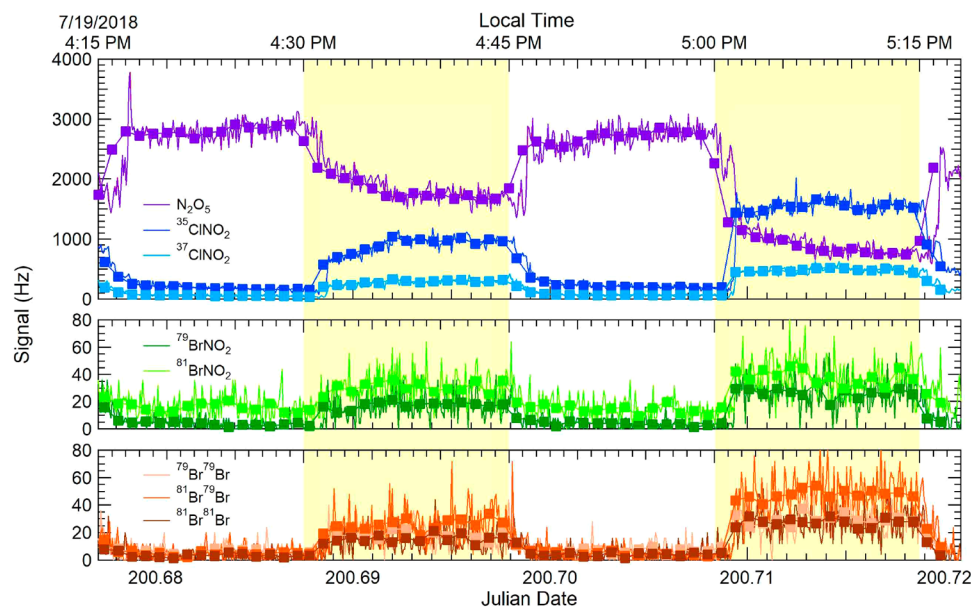


Figure 5. Example timeseries for N_2O_5 loss by particle modulation (top panel), ClNO_2 production (second panel), BrNO_2 production (third panel), and Br_2 production (bottom panel) for the Owens Lake “sediment” sample. Markers are minute-averaged data to enhance visual clarity. Tinted background indicates periods of N_2O_5 uptake onto aerosol.

containing salts with values of $\gamma_{\text{N}_2\text{O}_5} \sim 0.03$ and high values of $\varphi_{\text{ClNO}_2} (>0.5)$. One notable exception to this trend is the Salton Sea, which had the lowest values of $\gamma_{\text{N}_2\text{O}_5}$ (0.004–0.006) out of all the playas and somewhat low φ_{ClNO_2} (0.2–0.7) despite having a mass fraction of evaporites (49%) on par with other samples that have much higher values of $\gamma_{\text{N}_2\text{O}_5}$ and φ_{ClNO_2} . The Salton Sea is uniquely influenced by persistent anthropogenic activities, including agricultural runoff,¹¹² that influence the composition of the dust emitted from this sample.^{49,113} While particulate nitrate (NO_3^-), which has been shown to suppress N_2O_5 uptake via the “nitrate effect”,^{19,22} was not measured in significant concentrations (<0.4 wt %, see Table S4), organic compounds from pesticides, herbicides, fertilizers, and other anthropogenic sources are commonly found at the Salton Sea.¹¹⁴ Organic coatings have been shown to suppress $\gamma_{\text{N}_2\text{O}_5}$ ^{15,23,115–117} and φ_{ClNO_2} ⁴³ consistent with our low values of $\gamma_{\text{N}_2\text{O}_5}$ and φ_{ClNO_2} for the Salton Sea.

We also used the soluble inorganic ion content data as model input for ISORROPIA-II to estimate aerosol liquid water content and aqueous chloride concentration as a function of RH. These results were used to predict φ_{ClNO_2} from eq 3. The experimentally measured φ_{ClNO_2} values plotted against the chloride-to-water ratio evaluated by ISORROPIA-II are shown in Figure 4. This model is run in two ways: either insoluble compounds are allowed to precipitate, or aerosols are assumed to form only metastable solutions. Both modes gave similar results, and we show results using metastable solutions. φ_{ClNO_2} was overpredicted in all cases except two: Salt Flat and Sulphur Springs Draw. These two dust samples have the highest measured φ_{ClNO_2} values, are well-predicted by ISORROPIA-II and eq 3, and have values of $\gamma_{\text{N}_2\text{O}_5}$ consistent with deliquesced NaCl (see Figures 1 and 2 and Table S3). For other samples, the disagreement between our measurements and predictions shown in Figure 4 depends on several factors. The most obvious source of uncertainty is the aerosol phase. When predicting the aerosol liquid water content, carbonates and hydrates are not factored into current thermodynamic predictions; yet, these compounds have been suggested to be

important for explaining the water uptake and chemical properties of playa aerosols in previous studies.^{55,56} Neglecting these compounds would lead to underpredictions of liquid water content and overpredictions of ClNO_2 yields. Further, playa dust aerosol generation involves saltation and sand-blasting processes that can result in nonuniform distributions of evaporites within the aerosol population in terms of particle size. In this work, the inorganic ion content was not measured as a function of aerosol size, and thus the PM_1 used in our experiments has a different evaporite concentration and composition than the bulk inorganic ion data used to predict the liquid water content and yields of ClNO_2 .

The Lordsburg playa is the only sample for which ClNO_2 production was inefficient (~0.05–0.08); yet, ISORROPIA-II estimates a $\text{Cl}^-_{(\text{aq})}/\text{H}_2\text{O}_{(\text{l})}$ ratio high enough to efficiently generate ClNO_2 from eq 3. These results are best explained by the presence of silicates on the aerosol surface^{55,109} that dominate N_2O_5 uptake and limit the production of ClNO_2 . These competing reactions with silicates and other competitive nucleophiles, the suppressing effect of organic coatings, and the uptake and direct reaction of ClNO_2 in aqueous phase particles are not factored into eq 3 when predicting yields of ClNO_2 , which would lead to an overprediction of ClNO_2 by eq 3.¹¹⁸ The surface composition of the aerosol is also important when predicting yields of ClNO_2 .¹¹¹ Therefore, a critical look at how mineralogy and surface chemistry (for instance, organic coatings, clay coatings, or isolated evaporite structures on aerosol surfaces) affect both the reactivity of N_2O_5 and the production of competing products is warranted and will be the subject of a companion paper.

3.3. Production of Br_2 and BrNO_2 . In addition to ClNO_2 , appreciable amounts of molecular bromine (Br_2) were also detected when dust generated from the Owens Lake “sediment” and Sulphur Springs Draw samples was reacted with N_2O_5 (see Figures 1 and 5 and Table S3). φ_{Br_2} values from the Sulphur Springs Draw were too small to accurately quantify (<0.02) and were 0.054–0.07 from the Owens Lake “sediment” sample. Our Br_2 yields are surprisingly low

considering that measured chloride-to-bromide ratios (Cl^-/Br^-), by mass, were ~ 26 for Sulphur Springs Draw and ~ 46 for the Owens Lake “sediment” sample. We would expect similar yields of ClNO_2 and Br_2 of ~ 0.5 for both samples based on previous work.⁸⁴ Additionally, for Black Rock ($\text{Cl}^-/\text{Br}^- \sim 102$), Great Salt Lake ($\text{Cl}^-/\text{Br}^- \sim 77$), Owens Lake “crust” ($\text{Cl}^-:\text{Br}^- \sim 53$), and Lordsburg ($\text{Cl}^-/\text{Br}^- \sim 0.7$), some Br_2 production was expected. BrNO_2 was also observed in trace quantities when dust generated from the Owens Lake “sediment” sample was reacted with N_2O_5 (Figure 5). Although we could not quantify the yield of BrNO_2 (φ_{BrNO_2}) from this sample, this observation is still novel and represents, to our knowledge, the first observations of BrNO_2 production from playa dusts and the first observation of BrNO_2 produced during an AFT study from real aerosol sources as opposed to commercially available salt standards. The production of Br_2 and BrNO_2 from the Owens Lake “sediment” sample and our observation that φ_{ClNO_2} is less than unity further demonstrate the important role of competing nucleophiles, such as Br^- , when predicting yields of ClNO_2 .¹¹⁸

Br_2 is thought to be formed either by BrNO_2 reacting with excess bromide or via ClNO_2 reacting with bromide either to form BrNO_2 (the latter then reacting with bromide to form Br_2) or to form BrCl (that reacts further with bromide to form Br_2). We did not observe BrCl in any experiment, consistent with previous observations.^{84,119} Fickert et al., 1998¹¹⁹ demonstrated that when $\text{ClNO}_{2(g)}$ is taken up by dilute bromide solutions ($< 10^{-4}$ M), BrNO_2 is the dominant product, and for more concentrated solutions ($> 10^{-3}$ M), Br_2 production is favored. However, in the absence of ClNO_2 , Schweitzer et al., 1998¹²⁰ proposed that BrNO_2 efficiently reacts with Br^- to form Br_2 as a final product. We similarly observed Br_2 as the only detected gas-phase product in our AFT when using pure NaBr solutions (~ 0.002 M) likely because the aerosol bromide concentration was high enough to facilitate the conversion to Br_2 . Using the aerosol liquid water content predicted by ISOROPPIA-II, we predict a molar concentration of $[\text{Br}^-] \sim 10^{-6}$ M for all of our playa samples resulting in dilute Br^- solutions that should produce low yields of both BrNO_2 and Br_2 . It is still not entirely clear why the Owens Lake “sediment” produced appreciable Br_2 and BrNO_2 , whereas Sulphur Springs Draw produced only detectable Br_2 considering the Cl^-/Br^- and $[\text{Br}^-]$ were similar for both playa samples. Our best explanation is that a more concentrated solution of Br^- forms for the Sulphur Springs Draw sample than the Owens Lake “sediment” sample and that the higher φ_{ClNO_2} from the Sulphur Springs Draw would produce enough ClNO_2 to promote Br_2 formation via pathways described by Schweitzer et al., 1998 and Frenzel et al., 1998. Thus, prediction of the pathways for ClNO_2 production vs Br_2 production following reaction with N_2O_5 may not be as straightforward on playa surfaces compared to that of surfaces of simple brines and requires more in depth chemical knowledge beyond the Cl^-/Br^- value.

3.4. Atmospheric Implications. Our results demonstrate that saline dusts react efficiently with N_2O_5 to produce trace halogen gases in high yields, which are both important parameters for high production rates of ClNO_2 . During the NACHTT campaign, a recent study in Colorado where ClNO_2 was measured in an inland environment, playa dusts were speculated to contribute some of the observed inland budgets of ClNO_2 via an indirect production mechanism caused by the acid displacement of particulate chloride from supermicron

playa dust particles leading to the formation and partitioning of HCl to submicron particles that can then form ClNO_2 .⁶² Our results demonstrate that in addition to this indirect production mechanism, playa dusts are a potentially important source of particulate chloride that can also facilitate the direct production of ClNO_2 from reactions between N_2O_5 and submicron particles. The long-range transport of submicron playa dust particles to mountain and urban receptor sites has been observed,^{52,56,121} highlighting the atmospheric relevance of our laboratory studies. Future laboratory and field studies are warranted to determine the relative importance of direct and indirect production mechanisms of ClNO_2 from playa dusts in different inland environments.

Yields of ClNO_2 from N_2O_5 uptake are typically estimated to be a function of aerosol liquid water and chloride content;^{14,22,34} however, yields of ClNO_2 generated from playa dusts were typically overpredicted when only aerosol liquid water content and aqueous chloride were considered. We find that while some of the playa samples used in this work do behave like deliquesced NaCl , which is well-captured by this parameterization, most of our observed yields of ClNO_2 vary as a function of mineralogy and RH. It is likely that the mineral content, surface mineralogy, chemical composition, and the presence of hydrates play an important yet underappreciated role in determining the liquid water content and phase of particulate chloride present in playa dust aerosols (e.g., whether the chloride is aqueous or not) that is not captured in predictions of the ClNO_2 yield made using eq 3. Size-resolved differences in playa dust composition and reactions between minerals and N_2O_5 that compete with water and chloride resulting in a yield of ClNO_2 less than unity are also important considerations to accurately predict yields of ClNO_2 from saline dusts. Future work is needed to explore these mechanisms in detail on saline dust particles.

In addition to ClNO_2 , some of the samples also generated Br_2 and BrNO_2 when reacted with N_2O_5 . While halogen oxides (e.g., ClO and BrO) have been observed above playas,^{59–61,122,123} our measurements demonstrate the potential for playa dusts to generate halogenated trace gases at high yields following nighttime heterogeneous chemistry. Because Cl^- atoms are more reactive with VOCs (and facilitate O_3 production) while Br^- atoms are more reactive with O_3 (and destroy O_3), an understanding of the distribution of brominated and chlorinated products generated from playa dusts is important for modeling tropospheric O_3 concentrations.² The CMAQ model has recently been updated to consider the heterogeneous production of ClNO_2 from biomass burning aerosol, sea salts, and industrial sources of aerosols.⁴⁴ On the basis of our findings, saline dusts should also be incorporated in CMAQ and analogous models as an important source of particulate chloride, and the direct formation of ClNO_2 from submicron playa dust particles demonstrated herein should also be included in order to accurately quantify the impact of this chemistry on inland budgets of ClNO_2 and the subsequent impacts on tropospheric O_3 . Further, the spatial extent of playas and their emissions are expected to increase in the future as both salinization and aridification increase globally as a result of anthropogenic land use and water use practices.^{124–126} Our findings suggest that increased emissions from playas will significantly impact budgets of inland ClNO_2 and other reactive halogens with subsequent impacts on budgets of ground-level O_3 and regional air quality.

ASSOCIATED CONTENT

Supporting Information

The Supporting Information is available free of charge on the ACS Publications website at DOI: [10.1021/acs.est.9b01112](https://doi.org/10.1021/acs.est.9b01112).

Description of the playa samples, dust generation setup, gas-phase compound detection, and soluble ion detection; five figures (playa photos, playa locations, laboratory setup, representative aerosol size distributions, and example of linearity between S and k_{het}) and four tables (sample coordinates, corrections to S measurements, γ_{N2O5} and φ values for all samples, and IC data) are also included ([PDF](#))

AUTHOR INFORMATION

Corresponding Author

*E-mail: cgaston@rsmas.miami.edu. Phone: (305) 421-4979.

ORCID

Dhruv Mitroo: [0000-0002-7398-2020](#)

Thomas E. Gill: [0000-0001-9011-4105](#)

Kerri A. Pratt: [0000-0003-4707-2290](#)

Cassandra J. Gaston: [0000-0003-1383-8585](#)

Notes

The authors declare no competing financial interest.

ACKNOWLEDGMENTS

This research was supported by the National Science Foundation grants AGS-1663740 and AGS-1663726. S.H. and K.A.P. acknowledge the University of Michigan REU Program in the Chemical Sciences (CHE-1460990). We are very grateful to the following individuals for collection of samples: Prof. Heather Holmes and Prof. Bernhard Bach (Black Rock Desert playa); Prof. Maura Hahnberger (Great Salt Lake playa); Prof. Joanna Nield, Jana Lasser, and Lucas Goehring (Owens Lake playa); Prof. Junran Li (Salt Flat playa); Prof. Roya Bahreini (Salton Sea playa); Dr. R. Scott Van Pelt (Sulphur Springs Draw playa). Lordsburg playa samples were collected by T.E.G. We thank Mark Engle of the U.S. Geological Survey for insight on anthropogenic contributions to the Sulphur Springs Draw samples. We are indebted to Prof. Joel Thornton for use of the CIMS.

REFERENCES

- (1) Saiz-Lopez, A.; von Glasow, R. Reactive halogen chemistry in the troposphere. *Chem. Soc. Rev.* **2012**, *41* (19), 6448–6472.
- (2) Simpson, W. R.; Brown, S. S.; Saiz-Lopez, A.; Thornton, J. A.; von Glasow, R. Tropospheric Halogen Chemistry: Sources, Cycling, and Impacts. *Chem. Rev.* **2015**, *115* (10), 4035–4062.
- (3) Aschmann, S. M.; Atkinson, R. Rate Constants for the Gas-Phase Reactions of Alkanes with Cl Atoms at 296 ± 2 K. *Int. J. Chem. Kinet.* **1995**, *27* (6), 613–622.
- (4) Chang, S. Y.; Allen, D. T. Atmospheric chlorine chemistry in southeast Texas: Impacts on ozone formation and control. *Environ. Sci. Technol.* **2006**, *40* (1), 251–262.
- (5) Chang, S. Y.; McDonald-Buller, E.; Kimura, Y.; Yarwood, G.; Neece, J.; Russell, M.; Tanaka, P.; Allen, D. Sensitivity of urban ozone formation to chlorine emission estimates. *Atmos. Environ.* **2002**, *36* (32), 4991–5003.
- (6) Knipping, E. M.; Dabdub, D. Impact of chlorine emissions from sea-salt aerosol on coastal urban ozone. *Environ. Sci. Technol.* **2003**, *37* (2), 275–284.
- (7) Nelson, L.; Rattigan, O.; Neavyn, R.; Sidebottom, H.; Treacy, J.; Nielsen, O. J. Absolute and Relative Rate Constants for the Reactions of Hydroxyl Radicals and Chlorine Atoms with a Series of Aliphatic-
Alcohols and Ethers at 298-K. *Int. J. Chem. Kinet.* **1990**, *22* (11), 1111–1126.
- (8) Tanaka, P. L.; Riemer, D. D.; Chang, S. H.; Yarwood, G.; McDonald-Buller, E. C.; Apel, E. C.; Orlando, J. J.; Silva, P. J.; Jimenez, J. L.; Canagaratna, M. R.; Neece, J. D.; Mullins, C. B.; Allen, D. T. Direct evidence for chlorine-enhanced urban ozone formation in Houston, Texas. *Atmos. Environ.* **2003**, *37* (9–10), 1393–1400.
- (9) Wang, L.; Arey, J.; Atkinson, R. Reactions of chlorine atoms with a series of aromatic hydrocarbons. *Environ. Sci. Technol.* **2005**, *39* (14), 5302–5310.
- (10) Platt, U.; Honninger, G. The role of halogen species in the troposphere. *Chemosphere* **2003**, *52* (2), 325–38.
- (11) Finlayson-Pitts, B. J.; Ezell, M. J.; Pitts, J. N., Jr. Formation of chemically active chlorine compounds by reactions of atmospheric NaCl particles with gaseous N_2O_5 and $ClONO_2$. *Nature* **1989**, *337*, 241–244.
- (12) Osthoff, H. D.; Roberts, J. M.; Ravishankara, A. R.; Williams, E. J.; Lerner, B. M.; Sommariva, R.; Bates, T. S.; Coffman, D.; Quinn, P. K.; Dibb, J. E.; Stark, H.; Burkholder, J. B.; Talukdar, R. K.; Meagher, J.; Fehsenfeld, F. C.; Brown, S. S. High levels of nitryl chloride in the polluted subtropical marine boundary layer. *Nat. Geosci.* **2008**, *1* (5), 324–328.
- (13) Thornton, J. A.; Kercher, J. P.; Riedel, T. P.; Wagner, N. L.; Cozic, J.; Holloway, J. S.; Dube, W. P.; Wolfe, G. M.; Quinn, P. K.; Middlebrook, A. M.; Alexander, B.; Brown, S. S. A large atomic chlorine source inferred from mid-continental reactive nitrogen chemistry. *Nature* **2010**, *464* (7286), 271–274.
- (14) Behnke, W.; George, C.; Scheer, V.; Zetzsch, C. Production and decay of $ClNO_2$ from the reaction of gaseous N_2O_5 with NaCl solution: Bulk and aerosol experiments. *J. Geophys. Res.-Atmos.* **1997**, *102* (D3), 3795–3804.
- (15) Gaston, C. J.; Thornton, J. A.; Ng, N. L. Reactive uptake of N_2O_5 to internally mixed inorganic and organic particles: the role of organic carbon oxidation state and inferred organic phase separations. *Atmos. Chem. Phys.* **2014**, *14* (11), 5693–5707.
- (16) Hallquist, M.; Stewart, D. J.; Stephenson, S. K.; Cox, R. A. Hydrolysis of N_2O_5 on sub-micron sulfate aerosols. *Phys. Chem. Chem. Phys.* **2003**, *5* (16), 3453–3463.
- (17) Hu, J. H.; Abbatt, J. P. D. Reaction probabilities for N_2O_5 hydrolysis on sulfuric acid and ammonium sulfate aerosols at room temperature. *J. Phys. Chem. A* **1997**, *101* (5), 871–878.
- (18) Kane, S. M.; Caloz, F.; Leu, M. T. Heterogeneous uptake of gaseous N_2O_5 by $(NH_4)_2SO_4$, NH_4HSO_4 , and H_2SO_4 aerosols. *J. Phys. Chem. A* **2001**, *105* (26), 6465–6470.
- (19) Mentel, T. F.; Sohn, M.; Wahner, A. Nitrate effect in the heterogeneous hydrolysis of dinitrogen pentoxide on aqueous aerosols. *Phys. Chem. Chem. Phys.* **1999**, *1* (24), 5451–5457.
- (20) Mozurkewich, M.; Calvert, J. G. Reaction Probability of N_2O_5 on Aqueous Aerosols. *J. Geophys. Res.* **1988**, *93* (D12), 15889–15896.
- (21) Thornton, J. A.; Abbatt, J. P. D. N_2O_5 reaction on submicron sea salt aerosol: Kinetics, products, and the effect of surface active organics. *J. Phys. Chem. A* **2005**, *109* (44), 10004–10012.
- (22) Bertram, T. H.; Thornton, J. A. Toward a general parameterization of N_2O_5 reactivity on aqueous particles: the competing effects of particle liquid water, nitrate and chloride. *Atmos. Chem. Phys.* **2009**, *9* (21), 8351–8363.
- (23) McNeill, V. F.; Patterson, J.; Wolfe, G. M.; Thornton, J. A. The effect of varying levels of surfactant on the reactive uptake of N_2O_5 to aqueous aerosol. *Atmos. Chem. Phys.* **2006**, *6*, 1635–1644.
- (24) McDuffie, E. E.; Fibiger, D. L.; Dube, W. P.; Lopez-Hilfiker, F.; Lee, B. H.; Thornton, J. A.; Shah, V.; Jaegle, L.; Guo, H. Y.; Weber, R. J.; Reeves, J. M.; Weinheimer, A. J.; Schroder, J. C.; Campuzano-Jost, P.; Jimenez, J. L.; Dibb, J. E.; Veres, P.; Ebbes, C.; Sparks, T. L.; Wooldridge, P. J.; Cohen, R. C.; Hornbrook, R. S.; Apel, E. C.; Campos, T.; Hall, S. R.; Ullmann, K.; Brown, S. S. Heterogeneous N_2O_5 Uptake During Winter: Aircraft Measurements During the 2015 WINTER Campaign and Critical Evaluation of Current Parameterizations. *J. Geophys. Res.-Atmos.* **2018**, *123* (8), 4345–4372.

(25) Mielke, L. H.; Furgeson, A.; Odame-Ankrah, C. A.; Osthoff, H. D. Ubiquity of ClNO_2 in the urban boundary layer of Calgary, Alberta, Canada. *Can. J. Chem.* **2016**, *94* (4), 414–423.

(26) Mielke, L. H.; Furgeson, A.; Osthoff, H. D. Observation of ClNO_2 in a Mid-Continental Urban Environment. *Environ. Sci. Technol.* **2011**, *45* (20), 8889–8896.

(27) Riedel, T. P.; Wagner, N. L.; Dube, W. P.; Middlebrook, A. M.; Young, C. J.; Ozturk, F.; Bahreini, R.; VandenBoer, T. C.; Wolfe, D. E.; Williams, E. J.; Roberts, J. M.; Brown, S. S.; Thornton, J. A. Chlorine activation within urban or power plant plumes: Vertically resolved ClNO_2 and Cl_2 measurements from a tall tower in a polluted continental setting. *J. Geophys Res-Atmos* **2013**, *118* (15), 8702–8715.

(28) Tham, Y. J.; Wang, Z.; Li, Q. Y.; Wang, W. H.; Wang, X. F.; Lu, K. D.; Ma, N.; Yan, C.; Kecorius, S.; Wiedensohler, A.; Zhang, Y. H.; Wang, T. Heterogeneous N_2O_5 uptake coefficient and production yield of ClNO_2 in polluted northern China: roles of aerosol water content and chemical composition. *Atmos. Chem. Phys.* **2018**, *18* (17), 13155–13171.

(29) Wang, H. C.; Lu, K. D.; Guo, S.; Wu, Z. J.; Shang, D. J.; Tan, Z. F.; Wang, Y. J.; Le Breton, M.; Lou, S. R.; Tang, M. J.; Wu, Y. S.; Zhu, W. F.; Zheng, J.; Zeng, L. M.; Hallquist, M.; Hu, M.; Zhang, Y. H. Efficient N_2O_5 uptake and NO_3^- oxidation in the outflow of urban Beijing. *Atmos. Chem. Phys.* **2018**, *18* (13), 9705–9721.

(30) Wang, X. F.; Wang, H.; Xue, L. K.; Wang, T.; Wang, L. W.; Gu, R. R.; Wang, W. H.; Tham, Y. J.; Wang, Z.; Yang, L. X.; Chen, J. M.; Wang, W. X. Observations of N_2O_5 and ClNO_2 at a polluted urban surface site in North China: High N_2O_5 uptake coefficients and low ClNO_2 product yields. *Atmos. Environ.* **2017**, *156*, 125–134.

(31) Wang, Z.; Wang, W. H.; Tham, Y. J.; Li, Q. Y.; Wang, H.; Wen, L.; Wang, X. F.; Wang, T. Fast heterogeneous N_2O_5 uptake and ClNO_2 production in power plant and industrial plumes observed in the nocturnal residual layer over the North China Plain. *Atmos. Chem. Phys.* **2017**, *17* (20), 12361–12378.

(32) Yun, H.; Wang, T.; Wang, W. H.; Tham, Y. J.; Li, Q. Y.; Wang, Z.; Poon, S. C. N. Nighttime NO_x loss and ClNO_2 formation in the residual layer of a polluted region: Insights from field measurements and an iterative box model. *Sci. Total Environ.* **2018**, *622*, 727–734.

(33) Dentener, F. J.; Crutzen, P. J. Reaction of N_2O_5 on Tropospheric Aerosols - Impact on the Global Distributions of NO_x , O_3 , and OH . *J. Geophys Res-Atmos* **1993**, *98* (D4), 7149–7163.

(34) Roberts, J. M.; Osthoff, H. D.; Brown, S. S.; Ravishankara, A. R.; Coffman, D.; Quinn, P.; Bates, T. Laboratory studies of products of N_2O_5 uptake on Cl^- containing substrates. *Geophys. Res. Lett.* **2009**, *36*, L20808.

(35) Ganske, J. A.; Berko, H. N.; Finlayson-Pitts, B. J. Absorption Cross-Sections for Gaseous ClNO_2 and Cl_2 at 298-K - Potential Organic Oxidant Source in the Marine Troposphere. *J. Geophys. Res.* **1992**, *97* (D7), 7651–7656.

(36) Bannan, T. J.; Booth, A. M.; Bacak, A.; Muller, J. B. A.; Leather, K. E.; Le Breton, M.; Jones, B.; Young, D.; Coe, H.; Allan, J.; Visser, S.; Slowik, J. G.; Furger, M.; Prevot, A. S. H.; Lee, J.; Dunmore, R. E.; Hopkins, J. R.; Hamilton, J. F.; Lewis, A. C.; Whalley, L. K.; Sharp, T.; Stone, D.; Heard, D. E.; Fleming, Z. L.; Leigh, R.; Shallcross, D. E.; Percival, C. J. The first UK measurements of nitryl chloride using a chemical ionization mass spectrometer in central London in the summer of 2012, and an investigation of the role of Cl atom oxidation. *J. Geophys Res-Atmos* **2015**, *120* (11), 5638–5657.

(37) Mielke, L. H.; Stutz, J.; Tsai, C.; Hurlock, S. C.; Roberts, J. M.; Veres, P. R.; Froyd, K. D.; Hayes, P. L.; Cubison, M. J.; Jimenez, J. L.; Washenfelder, R. A.; Young, C. J.; Gilman, J. B.; de Gouw, J. A.; Flynn, J. H.; Grossberg, N.; Lefer, B. L.; Liu, J.; Weber, R. J.; Osthoff, H. D. Heterogeneous formation of nitryl chloride and its role as a nocturnal NO_x reservoir species during CalNex-LA 2010. *J. Geophys Res-Atmos* **2013**, *118* (18), 10638–10652.

(38) Phillips, G. J.; Tang, M. J.; Thieser, J.; Brickwedde, B.; Schuster, G.; Bohn, B.; Lelieveld, J.; Crowley, J. N. Significant concentrations of nitryl chloride observed in rural continental Europe associated with the influence of sea salt chloride and anthropogenic emissions. *Geophys. Res. Lett.* **2012**, *39*, L10811.

(39) Riedel, T. P.; Bertram, T. H.; Crisp, T. A.; Williams, E. J.; Lerner, B. M.; Vlasenko, A.; Li, S. M.; Gilman, J.; de Gouw, J.; Bon, D. M.; Wagner, N. L.; Brown, S. S.; Thornton, J. A. Nitryl Chloride and Molecular Chlorine in the Coastal Marine Boundary Layer. *Environ. Sci. Technol.* **2012**, *46* (19), 10463–10470.

(40) Tham, Y. J.; Yan, C.; Xue, L. K.; Zha, Q. Z.; Wang, X. F.; Wang, T. Presence of high nitryl chloride in Asian coastal environment and its impact on atmospheric photochemistry. *Chin. Sci. Bull.* **2014**, *59* (4), 356–359.

(41) Wagner, N. L.; Riedel, T. P.; Roberts, J. M.; Thornton, J. A.; Angevine, W. M.; Williams, E. J.; Lerner, B. M.; Vlasenko, A.; Li, S. M.; Dube, W. P.; Coffman, D. J.; Bon, D. M.; de Gouw, J. A.; Kuster, W. C.; Gilman, J. B.; Brown, S. S. The sea breeze/land breeze circulation in Los Angeles and its influence on nitryl chloride production in this region. *J. Geophys Res-Atmos* **2012**, *117*, D00V24.

(42) Kercher, J. P.; Riedel, T. P.; Thornton, J. A. Chlorine activation by N_2O_5 : simultaneous, in situ detection of ClNO_2 and N_2O_5 by chemical ionization mass spectrometry. *Atmos. Meas. Tech.* **2009**, *2* (1), 193–204.

(43) Ryder, O. S.; Campbell, N. R.; Shaloski, M.; Al-Mashat, H.; Nathanson, G. M.; Bertram, T. H. Role of Organics in Regulating ClNO_2 Production at the Air-Sea Interface. *J. Phys. Chem. A* **2015**, *119* (31), 8519–8526.

(44) Sarwar, G.; Simon, H.; Xing, J.; Mathur, R. Importance of tropospheric ClNO_2 chemistry across the Northern Hemisphere. *Geophys. Res. Lett.* **2014**, *41* (11), 4050–4058.

(45) Ahern, A. T.; Goldberger, L.; Jahl, L.; Thornton, J.; Sullivan, R. C. Production of N_2O_5 and ClNO_2 through Nocturnal Processing of Biomass-Burning Aerosol. *Environ. Sci. Technol.* **2018**, *52* (2), 550–559.

(46) Kolesar, K. R.; Mattson, C. N.; Peterson, P. K.; May, N. W.; Prendergast, R. K.; Pratt, K. A. Increases in wintertime $\text{PM}_{2.5}$ sodium and chloride linked to snowfall and road salt application. *Atmos. Environ.* **2018**, *177*, 195–202.

(47) Lee, B. H.; Lopez-Hilfiker, F. D.; Schroder, J. C.; Campuzano-Jost, P.; Jimenez, J. L.; McDuffie, E. E.; Fibiger, D. L.; Veres, P. R.; Brown, S. S.; Campos, T. L.; Weinheimer, A. J.; Flocke, F. F.; Norris, G.; O'Mara, K.; Green, J. R.; Fiddler, M. N.; Bililign, S.; Shah, V.; Jaegle, L.; Thornton, J. A. Airborne Observations of Reactive Inorganic Chlorine and Bromine Species in the Exhaust of Coal-Fired Power Plants. *J. Geophys Res-Atmos* **2018**, *123* (19), 11225–11237.

(48) Abuduwaili, J.; Gabchenko, M. V.; Xu, J. R. Eolian transport of salts - A case study in the area of Lake Ebinur (Xinjiang, Northwest China). *J. Arid Environ.* **2008**, *72* (10), 1843–1852.

(49) Buck, B. J.; King, J.; Etyemezian, V. Effects of Salt Mineralogy on Dust Emissions, Salton Sea, California. *Soil Sci. Soc. Am. J.* **2011**, *75* (5), 1971–1985.

(50) Cahill, T. A.; Gill, T. E.; Reid, J. S.; Gearhart, E. A.; Gillette, D. A. Saltating particles, playa crusts and dust aerosols at Owens (dry) Lake, California. *Earth Surf. Processes Landforms* **1996**, *21* (7), 621–639.

(51) Gill, T. E.; Gillette, D. A.; Niemeyer, T.; Winn, R. T. Elemental geochemistry of wind-erodible playa sediments, Owens Lake, California. *Nucl. Instrum. Methods Phys. Res., Sect. B* **2002**, *189*, 209–213.

(52) Niemeyer, T. C.; Gillette, D. A.; Deluisi, J. J.; Kim, Y. J.; Niemeyer, W. F.; Ley, T.; Gill, T. E.; Ono, D. Optical depth, size distribution and flux of dust from Owens Lake, California. *Earth Surf. Processes Landforms* **1999**, *24* (5), 463–479.

(53) Reynolds, R. L.; Yount, J. C.; Reheis, M.; Goldstein, H.; Chavez, P.; Fulton, R.; Whitney, J.; Fuller, C.; Forester, R. M. Dust emission from wet and dry playas in the Mojave desert, USA. *Earth Surf. Processes Landforms* **2007**, *32* (12), 1811–1827.

(54) Rosen, M. R., The importance of groundwater in playas: A review of playa classifications and the sedimentology and hydrology of playas. In *Paleoclimate and Basin Evolution of Playa Systems*, Rosen, M. R., Ed. Geological Society of America: Boulder, CO, 1994; Special Paper 289, 1–18.

(55) Gaston, C. J.; Pratt, K. A.; Suski, K. J.; May, N. W.; Gill, T. E.; Prather, K. A. Laboratory Studies of the Cloud Droplet Activation Properties and Corresponding Chemistry of Saline Playa Dust. *Environ. Sci. Technol.* **2017**, *51* (3), 1348–1356.

(56) Pratt, K. A.; Twohy, C. H.; Murphy, S. M.; Moffet, R. C.; Heymsfield, A. J.; Gaston, C. J.; DeMott, P. J.; Field, P. R.; Henn, T. R.; Rogers, D. C.; Gilles, M. K.; Seinfeld, J. H.; Prather, K. A. Observation of playa salts as nuclei in orographic wave clouds. *J. Geophys. Res.* **2010**, *115*, D15301.

(57) Bullard, J. E.; Harrison, S. P.; Baddock, M. C.; Drake, N.; Gill, T. E.; McTainsh, G.; Sun, Y. B. Preferential dust sources: A geomorphological classification designed for use in global dust-cycle models. *J. Geophys. Res.* **2011**, *116*, F04034.

(58) Ginoux, P.; Prospero, J. M.; Gill, T. E.; Hsu, N. C.; Zhao, M. Global-Scale Attribution of Anthropogenic and Natural Dust Sources and Their Emission Rates Based on MODIS Deep Blue Aerosol Products. *Rev. Geophys.* **2012**, *50*, RG3005.

(59) Stutz, J.; Ackermann, R.; Fast, J. D.; Barrie, L. Atmospheric reactive chlorine and bromine at the Great Salt Lake, Utah. *Geophys. Res. Lett.* **2002**, *29* (10), 1380.

(60) Honninger, G.; Bobrowski, N.; Palenque, E. R.; Torrez, R.; Platt, U. Reactive bromine and sulfur emissions at Salar de Uyuni, Bolivia. *Geophys. Res. Lett.* **2004**, *31* (4), L04101.

(61) Hebestreit, K.; Stutz, J.; Rosen, D.; Matveiv, V.; Peleg, M.; Luria, M.; Platt, U. DOAS measurements of tropospheric bromine oxide in mid-latitudes. *Science* **1999**, *283* (5398), 55–57.

(62) Jordan, C. E.; Pszenny, A. A. P.; Keene, W. C.; Cooper, O. R.; Deegan, B.; Maben, J.; Routhier, M.; Sander, R.; Young, A. H. Origins of aerosol chlorine during winter over north central Colorado, USA. *J. Geophys. Res.-Atmos.* **2015**, *120* (2), 678–694.

(63) Brown, S. S.; Thornton, J. A.; Keene, W. C.; Pszenny, A. A. P.; Sive, B. C.; Dube, W. P.; Wagner, N. L.; Young, C. J.; Riedel, T. P.; Roberts, J. M.; VandenBoer, T. C.; Bahreini, R.; Ozturk, F.; Middlebrook, A. M.; Kim, S.; Hubler, G.; Wolfe, D. E. Nitrogen, Aerosol Composition, and Halogens on a Tall Tower (NACHTT): Overview of a wintertime air chemistry field study in the front range urban corridor of Colorado. *J. Geophys. Res.-Atmos.* **2013**, *118* (14), 8067–8085.

(64) Young, A. H.; Keene, W. C.; Pszenny, A. A. P.; Sander, R.; Thornton, J. A.; Riedel, T. P.; Maben, J. R. Phase partitioning of soluble trace gases with size-resolved aerosols in near-surface continental air over northern Colorado, USA, during winter. *J. Geophys. Res.-Atmos.* **2013**, *118* (16), 9414–9427.

(65) Adams, K. D.; Sada, D. W. Surface water hydrology and geomorphic characterization of a playa lake system: Implications for monitoring the effects of climate change. *J. Hydrol.* **2014**, *510*, 92–102.

(66) Engelbrecht, J. P.; Moosmuller, H.; Pincock, S.; Jayanty, R. K. M.; Lersch, T.; Casuccio, G. Technical note: Mineralogical, chemical, morphological, and optical interrelationships of mineral dust suspensions. *Atmos. Chem. Phys.* **2016**, *16* (17), 10809–10830.

(67) Lewis, J. M.; Kaplan, M. L.; Vellore, R.; Rabin, R. M.; Hallett, J.; Cohn, S. A. Dust storm over the Black Rock Desert: Larger-scale dynamic signatures. *J. Geophys. Res.* **2011**, *116*, D06113.

(68) Tollerud, H. J.; Fantle, M. S. The temporal variability of centimeter-scale surface roughness in a playa dust source: Synthetic aperture radar investigation of playa surface dynamics. *Remote Sens. Environ.* **2014**, *154*, 285–297.

(69) Hahnenberger, M.; Nicoll, K. Geomorphic and land cover identification of dust sources in the eastern Great Basin of Utah, USA. *Geomorphology* **2014**, *204*, 657–672.

(70) Rivera Rivera, N. I.; Gill, T. E.; Bleiweiss, M. P.; Hand, J. L. Source characteristics of hazardous Chihuahuan Desert dust outbreaks. *Atmos. Environ.* **2010**, *44* (20), 2457–2468.

(71) Klose, M.; Gill, T. E.; Webb, N. P.; Van Zee, J. W. Field sampling of loose erodible material: A new system to consider the full particle-size spectrum. *Aeolian Res.* **2017**, *28*, 83–90.

(72) Cahill, T. A.; Gillette, D. A.; Gill, T. E.; Gearhart, E. A.; Reid, J. S.; Yau, M. L. *Earth Surf. Processes Landforms* **1994**, *21*, A-132–105.

(73) Gill, T. E.; Gillette, D. A. Owens Lake: A natural laboratory for aridification, playa desiccation and desert dust. *Nucl. Instrum. Methods Phys. Res., Sect. B* **1991**, *24* (9), 432.

(74) Reheis, M. C. Dust deposition downwind of Owens (dry) Lake, 1991–1994: Preliminary findings. *J. Geophys. Res.-Atmos.* **1997**, *102* (D22), 25999–26008.

(75) Perez, A. E.; Gill, T. E. Salt Flat Basin's Contribution to Regional Dust Production and Potential Influence on Dry Deposition in the Guadalupe Mountains (Texas, USA). *Natural Resources and Environmental Issues* **2009**, *15* (1), 117–118.

(76) Frie, A. L.; Dingle, J. H.; Ying, S. C.; Bahreini, R. The Effect of a Receding Saline Lake (The Salton Sea) on Airborne Particulate Matter Composition. *Environ. Sci. Technol.* **2017**, *51* (15), 8283–8292.

(77) Li, J.; Kandakji, T.; Lee, J. A.; Tatarko, J.; Blackwell, J.; Gill, T. E.; Collins, J. D. Blowing dust and highway safety in the southwestern United States: Characteristics of dust emission “hotspots” and management implications. *Sci. Total Environ.* **2018**, *621*, 1023–1032.

(78) Frederick, C. D. Late Quaternary clay dune sedimentation on the Llano Estacado, Texas. *Plains Anthropol.* **1998**, *43* (164), 137–155.

(79) Lafon, S.; Alfaro, S. C.; Chevaillier, S.; Rajot, J. L. A new generator for mineral dust aerosol production from soil samples in the laboratory: GAMEL. *Aeolian Res.* **2014**, *15*, 319–334.

(80) Sullivan, R. C.; Moore, M. J. K.; Petters, M. D.; Kreidenweis, S. M.; Roberts, G. C.; Prather, K. A. Effect of chemical mixing state on the hygroscopicity and cloud nucleation properties of calcium mineral dust particles. *Atmos. Chem. Phys.* **2009**, *9* (10), 3303–3316.

(81) Gomes, L.; Bergametti, G.; Coude-Gaussen, G.; Rognon, P. Submicron Desert Dusts - a Sandblasting Process. *J. Geophys. Res.* **1990**, *95* (D9), 13927–13935.

(82) Vlasenko, A.; Sjogren, S.; Weingartner, E.; Gaggeler, H. W.; Ammann, M. Generation of submicron Arizona test dust aerosol: Chemical and hygroscopic properties. *Aerosol Sci. Technol.* **2005**, *39* (5), 452–460.

(83) Bertram, T. H.; Thornton, J. A.; Riedel, T. P. An experimental technique for the direct measurement of N_2O_5 reactivity on ambient particles. *Atmos. Meas. Tech.* **2009**, *2* (1), 231–242.

(84) Lopez-Hilfiker, F. D.; Constantin, K.; Kercher, J. P.; Thornton, J. A. Temperature dependent halogen activation by N_2O_5 reactions on halide-doped ice surfaces. *Atmos. Chem. Phys.* **2012**, *12* (11), 5237–5247.

(85) Wolfe, G. M.; Thornton, J. A.; McNeill, V. F.; Jaffe, D. A.; Reidmiller, D.; Chand, D.; Smith, J.; Swartzendruber, P.; Flocke, F.; Zheng, W. Influence of trans-Pacific pollution transport on acyl peroxy nitrate abundances and speciation at Mount Bachelor Observatory during INTEX-B. *Atmos. Chem. Phys.* **2007**, *7* (20), 5309–5325.

(86) Fuchs, N. A.; Sutugin, A. G. *Highly Dispersed Aerosols*; Ann Arbor Science: 1970.

(87) Brown, R. L. Tubular Flow Reactors with 1st-Order Kinetics. *J. Res. Natl. Bur. Stand.* **1978**, *83* (1), 1–8.

(88) DeCarlo, P. F.; Slowik, J. G.; Worsnop, D. R.; Davidovits, P.; Jimenez, J. L. Particle morphology and density characterization by combined mobility and aerodynamic diameter measurements. Part 1: Theory. *Aerosol Sci. Technol.* **2004**, *38* (12), 1185–1205.

(89) Tang, I. N.; Tridico, A. C.; Fung, K. H. Thermodynamic and optical properties of sea salt aerosols. *J. Geophys. Res.-Atmos.* **1997**, *102* (D19), 23269–23275.

(90) Wagner, C.; Schuster, G.; Crowley, J. N. An aerosol flow tube study of the interaction of N_2O_5 with calcite, Arizona dust and quartz. *Atmos. Environ.* **2009**, *43* (32), 5001–5008.

(91) Lopez-Hilfiker, F. D.; Iyer, S.; Mohr, C.; Lee, B. H.; D'Ambro, E. L.; Kurten, T.; Thornton, J. A. Constraining the sensitivity of iodide adduct chemical ionization mass spectrometry to multifunctional organic molecules using the collision limit and thermodynamic stability of iodide ion adducts. *Atmos. Meas. Tech.* **2016**, *9* (4), 1505–1512.

(92) Fountoukis, C.; Nenes, A. ISORROPIA II: a computationally efficient thermodynamic equilibrium model for K^+ - Ca^{2+} - Mg^{2+} - NH_4^+ - Na^+ - SO_4^{2-} - NO_3^- - Cl^- - H_2O aerosols. *Atmos. Chem. Phys.* **2007**, *7* (17), 4639–4659.

(93) Guo, L. Y.; Gu, W. J.; Peng, C.; Wang, W. G.; Li, Y. J.; Zong, T. M.; Tang, Y. J.; Wu, Z. J.; Lin, Q. H.; Ge, M. F.; Zhang, G. H.; Hu, M.; Bi, X. H.; Wang, X. M.; Tang, M. J. A comprehensive study of hygroscopic properties of calcium- and magnesium-containing salts: implication for hygroscopicity of mineral dust and sea salt aerosols. *Atmos. Chem. Phys.* **2019**, *19* (4), 2115–2133.

(94) Mogili, P. K.; Kleiber, P. D.; Young, M. A.; Grassian, V. H. N_2O_5 hydrolysis on the components of mineral dust and sea salt aerosol: Comparison study in an environmental aerosol reaction chamber. *Atmos. Environ.* **2006**, *40* (38), 7401–7408.

(95) Tang, M. J.; Schuster, G.; Crowley, J. N. Heterogeneous reaction of N_2O_5 with Illite and Arizona test dust particles. *Atmos. Chem. Phys.* **2014**, *14* (1), 245–254.

(96) Tang, M. J.; Thieser, J.; Schuster, G.; Crowley, J. N. Kinetics and mechanism of the heterogeneous reaction of N_2O_5 with mineral dust particles. *Phys. Chem. Chem. Phys.* **2012**, *14* (24), 8551–8561.

(97) Braun, C.; Krieger, U. K. Two dimensional angular light scattering in aqueous $NaCl$ single aerosol particles during deliquescence and efflorescence. *Opt. Express* **2001**, *8* (6), 314–321.

(98) Cziczo, D. J.; Abbatt, J. P. D. Infrared observations of the response of $NaCl$, $MgCl_2$, NH_4HSO_4 , and NH_4NO_3 aerosols to changes in relative humidity from 298 to 238 K. *J. Phys. Chem. A* **2000**, *104* (10), 2038–2047.

(99) Crowley, J. K. Visible and near-Infrared (0.4–2.5 μm) Reflectance Spectra of Playa Evaporite Minerals. *J. Geophys. Res.* **1991**, *96* (B10), 16231–16240.

(100) Koehler, K. A.; Kreidenweis, S. M.; DeMott, P. J.; Prenni, A. J.; Petters, M. D. Potential impact of Owens (dry) Lake dust on warm and cold cloud formation. *J. Geophys. Res.* **2007**, *112*, D12210.

(101) Abbatt, J. P. D.; Lee, A. K. Y.; Thornton, J. A. Quantifying trace gas uptake to tropospheric aerosol: recent advances and remaining challenges. *Chem. Soc. Rev.* **2012**, *41* (19), 6555–6581.

(102) Griffiths, P. T.; Badger, C. L.; Cox, R. A.; Folkers, M.; Henk, H. H.; Mentel, T. F. Reactive Uptake of N_2O_5 by Aerosols Containing Dicarboxylic Acids. Effect of Particle Phase, Composition, and Nitrate Content. *J. Phys. Chem. A* **2009**, *113* (17), 5082–5090.

(103) Thornton, J. A.; Braban, C. F.; Abbatt, J. P. D. N_2O_5 hydrolysis on sub-micron organic aerosols: the effect of relative humidity, particle phase, and particle size. *Phys. Chem. Chem. Phys.* **2003**, *5* (20), 4593–4603.

(104) Rojo, L.; Barnes, M. A.; Gill, T. E. Intercomparison of PIXE and ICP-AES Analyses of Aeolian Dust from Owens (Dry) Lake, California. *Geostand. Geoanal. Res.* **2012**, *36* (1), 83–102.

(105) Rojo, L.; Gill, T. E.; Gillette, D. A. Particle size/composition relationships of wind-eroding sediments, Owens (dry) Lake, California, USA. *X-Ray Spectrom.* **2008**, *37* (2), 111–115.

(106) Sweeney, M. R.; McDonald, E. V.; Etyemezian, V. Quantifying dust emissions from desert landforms, eastern Mojave Desert, USA. *Geomorphology* **2011**, *135* (1–2), 21–34.

(107) Messaoudi, S.; Bejaoui, B.; Akroud, F.; Hassen, M. B.; Sammari, C. Exploration of the reactivity of N_2O_5 with two $Si(OH)_4$ monomers using electronic structure methods. *Int. J. Quantum Chem.* **2013**, *113* (11), 1633–1640.

(108) Seisel, S.; Borensen, C.; Vogt, R.; Zellner, R. Kinetics and mechanism of the uptake of N_2O_5 on mineral dust at 298 K. *Atmos. Chem. Phys.* **2005**, *5*, 3423–3432.

(109) Hibbs, B.; Lee, M. M.; Hawley, J. W.; Kennedy, J. F. Some notes on the hydrogeology and ground-water quality of the Animas Basin system, southwestern New Mexico. *New Mexico Geol Soc. Fall Field Conf Guidebook* **2000**, *51*, 227–234.

(110) Hoffman, R. C.; Gebel, M. E.; Fox, B. S.; Finlayson-Pitts, B. J. Knudsen cell studies of the reactions of N_2O_5 and $ClONO_2$ with $NaCl$: development and application of a model for estimating available surface areas and corrected uptake coefficients. *Phys. Chem. Chem. Phys.* **2003**, *5* (9), 1780–1789.

(111) Gaston, C. J.; Thornton, J. A. Reacto-Diffusive Length of N_2O_5 in Aqueous Sulfate- and Chloride-Containing Aerosol Particles. *J. Phys. Chem. A* **2016**, *120* (7), 1039–1045.

(112) Robertson, D. M.; Schladow, S. G.; Holdren, G. C. Long-term changes in the phosphorus loading to and trophic state of the Salton Sea, California. *Hydrobiologia* **2008**, *604*, 21–36.

(113) Vogl, R. A.; Henry, R. N. Characteristics and contaminants of the Salton Sea sediments. *Hydrobiologia* **2002**, *473* (1–3), 47–54.

(114) Setmire, J. G.; Schroeder, R. A., Selenium and salinity concerns in the Salton Sea area. In *Environmental Chemistry of Selenium*, Frankenberger, Jr., W. T., Engberg, R. A., Eds.; Marcel Dekker, Inc.: New York, 1998, 205–221.

(115) Anttila, T.; Kiendler-Scharr, A.; Tillmann, R.; Mentel, T. F. On the reactive uptake of gaseous compounds by organic-coated aqueous aerosols: Theoretical analysis and application to the heterogeneous hydrolysis of N_2O_5 . *J. Phys. Chem. A* **2006**, *110* (35), 10435–10443.

(116) Escoria, E. N.; Sjostedt, S. J.; Abbatt, J. P. D. Kinetics of N_2O_5 Hydrolysis on Secondary Organic Aerosol and Mixed Ammonium Bisulfate-Secondary Organic Aerosol Particles. *J. Phys. Chem. A* **2010**, *114* (50), 13113–13121.

(117) Folkers, M.; Mentel, T. F.; Wahner, A. Influence of an organic coating on the reactivity of aqueous aerosols probed by the heterogeneous hydrolysis of N_2O_5 . *Geophys. Res. Lett.* **2003**, *30* (12), 1644.

(118) McDuffie, E. E.; Fibiger, D. L.; Dube, W. P.; Hilfiker, F. L.; Lee, B. H.; Jaegle, L.; Guo, H. Y.; Weber, R. J.; Reeves, J. M.; Weinheimer, A. J.; Schroder, J. C.; Campuzano-Jost, P.; Jimenez, J. L.; Dibb, J. E.; Veres, P.; Ebbesen, C.; Sparks, T. L.; Wooldridge, P. J.; Cohen, R. C.; Campos, T.; Hall, S. R.; Ullmann, K.; Roberts, J. M.; Thornton, J. A.; Brown, S. S. $ClNO_2$ Yields From Aircraft Measurements During the 2015 WINTER Campaign and Critical Evaluation of the Current Parameterization. *J. Geophys. Res.: Atmos.* **2018**, *123* (22), 12994–13015.

(119) Fickert, S.; Helleis, F.; Adams, J. W.; Moortgat, G. K.; Crowley, J. N. Reactive uptake of $ClNO_2$ on aqueous bromide solutions. *J. Phys. Chem. A* **1998**, *102* (52), 10689–10696.

(120) Schweitzer, F.; Mirabel, P.; George, C. Multiphase chemistry of N_2O_5 , $ClNO_2$, and $BrNO_2$. *J. Phys. Chem. A* **1998**, *102* (22), 3942–3952.

(121) Skiles, S. M.; Mallia, D. V.; Hallar, A. G.; Lin, J. C.; Lambert, A.; Petersen, R.; Clark, S. Implications of a shrinking Great Salt Lake for dust on snow deposition in the Wasatch Mountains, UT, as informed by a source to sink case study from the 13–14 April 2017 dust event. *Environ. Res. Lett.* **2018**, *13* (12), 124031.

(122) Tas, E.; Peleg, M.; Matveev, V.; Zingler, J.; Luria, M. Frequency and extent of bromine oxide formation over the Dead Sea. *Atmos. Environ.* **2005**, *110*, D11304.

(123) Matveev, V.; Peleg, M.; Rosen, D.; Tov-Alper, D. S.; Hebestreit, K.; Stutz, J.; Platt, U.; Blake, D.; Luria, M. Bromine oxide - ozone interaction over the Dead Sea. *J. Geophys. Res.-Atmos.* **2001**, *106* (D10), 10375–10387.

(124) AghaKouchak, A.; Norouzi, H.; Madani, K.; Mirchi, A.; Azarderakhsh, M.; Nazemi, A.; Nasrollahi, N.; Farahmand, A.; Mehran, A.; Hasanzadeh, E. Aral Sea syndrome desiccates Lake Urmia: Call for action. *J. Great Lakes Res.* **2015**, *41* (1), 307–311.

(125) Pelletier, J. D. Sensitivity of playa windblown-dust emissions to climatic and anthropogenic change. *J. Arid Environ.* **2006**, *66* (1), 62–75.

(126) Wang, J. D.; Song, C. Q.; Reager, J. T.; Yao, F. F.; Famiglietti, J. S.; Sheng, Y. W.; MacDonald, G. M.; Brun, F.; Schmied, H. M.; Marston, R. A.; Wada, Y. Recent global decline in endorheic basin water storages. *Nat. Geosci.* **2018**, *11* (12), 926–932.